Journal of the European Ceramic Society 17 (1997) 101–108

PII: S0955-2219(96)00070-2
0955-2219/97/$17.00

The Orientation of Binders and Particles During Ceramic Injection Moulding

T. Zhang,* S. Blackburn† & J. Bridgwater‡

IRC in Materials for High Performance Applications and School of Chemical Engineering, The University of Birmingham, Edgbaston, Birmingham B15 2TT, UK

(Received 22 January 1996; revised version received 21 March 1996; accepted 28 March 1996)

Abstract

By annealing sections of thick, injection-moulded ceramics, the orientation of the organic binder was studied. A modified calculation method for X-ray diffraction analysis was used for evaluation of particle orientation. Using a finite difference method, the temperature distribution in a mould system was related to the structure found. Fine plate-like particles became highly oriented during injection moulding and the oriented particles restricted the binder orientation and subsequent relaxation of the extended chains. © 1996 Elsevier Science Limited.

1 Introduction

When shear stress is applied to a polymer molecule or to a rigid non-spherical particle, each will orient; the polymer chain will extend or elongate while the rigid particle will rotate and adopt a preferred orientation. In ceramics the non-spherical particles may be fibres, whiskers or plate-like particles such as silicon carbide, alumina and clays. The degree and nature of the orientation will depend on the shear history and the properties of the components of the mixture.

A polymer is composed of an entangled mass of long-chain molecules which, during extrusion or injection moulding, become highly ordered by stretching. Frequently these chains lie parallel to the die or mould surface. Orientation can have a significant influence on the mechanical and thermal properties of the product. In conventional processing the orientation is largely uncontrolled, but oscillatory moulding processes[1] have been developed to induce controlled and desired orientation.

*School of Engineering Systems and Design, South Bank University, London SE1 0AA, UK.
†To whom correspondence should be addressed.
‡Department of Chemical Engineering, University of Cambridge, Pembroke Street, Cambridge CB2 3RA, UK.

During the plastic forming of ceramic powders, the shear stress will not change the shape of the particles due to the high elastic modulus, but will cause particle orientation. Cox and Williamson[2] have compared the effect of casting, spreading and extrusion on the orientation in ball-clays. Linear drying and sintering shrinkages were used to judge the orientation of the particles. It was found that all these processing methods developed planar particle orientation. In the manufacture of electronic ceramics, grain orientation is used to improve material performance,[3] e.g. bismuth titanate in tape casting and hot-pressing.[4,5] The effects of binder and powder content were investigated in the study but only related to the surface of thin films (<1 mm).

In the fabrication of structural ceramics, composites reinforced by fibres, whiskers and platelets are receiving great attention. In these, the degree of reinforcement is dependent on the orientation of the reinforcing phase. Hoffmann *et al.*[6] have studied the orientation of SiC whiskers in silicon nitride formed by slip casting. It was found that the orientation of the whiskers varied with the casting parameters as well as position in the sample. Tsao and Danforth[7] have also noted that the degree of orientation of whiskers in an extruded cylinder varied significantly from the centre to the surface. Chou and Green[8] have compared the orientation of silicon carbide platelets in the surface of reinforced alumina composites formed by slip casting, tape casting and dry compaction. It was shown that all of these processing routes produced an oriented structure and that orientation in ceramic components depended on the processing history and material frictional properties. Orientation also varied with the position within the component. These aspects are important as the control of microstructure in composite materials improves mechanical properties.

Recently, injection moulding has received great attention in ceramic forming because it offers opportunities for the cost-effective production of

complex parts in high-performance engineering materials.[9,10] In principle, there are similarities between injection moulding, slip casting and extrusion. During the moulding process, the material undergoes shearing, compression and cooling. The shear stress will develop an oriented microstructure of both the binder and the particles of the system. This may be one of the primary causes of anisotropic thermal expansion and the development of defects during debinding and sintering.[11,12] For successful moulding the process will be required to control orientation. This relies on the development of a sound understanding of the mechanism influencing the orientation process. Here we report on the orientation in large-section injection-moulded bars, relating the results to the shear and cooling history of the moulded body.

2 Experimental Details

2.1 Materials

The ceramic powders used were Baco RA107LS (Alcan Chemicals Ltd, UK; d_{50} = 0·5 μm) and F1500 (Universal Abrasives Ltd, UK; d_{50} = 2·9 μm). As shown in Fig. 1, the RA107LS powder contains a high proportion of tabular particles, typical of chemically derived aluminas; the F1500 powder is more angular, reflecting its formation by fusion and comminution. The binder system used was based on a mixture of ethylene–vinyl acetate copolymer (EVA) (grade Elvax 140 W, Du Pont) and paraffin wax (PW) (grade 130/135 FR, Shell Industrial Chemicals). To this system were added the moulding aids stearic acid (SA) and dibutylphthalate (DBP) (both from BDH Chemicals). The moulding compositions are summarized in Table 1.

Mixing was carried out in a Werner and Pfleiderer Z-blade mixer. The water circulation temperature of 90°C was controlled by an HB-150 M temperature controller (Grossenbacher Apparatebau AG, Switzerland). Mixing was continued for 1 h.

2.2 Moulding conditions

Moulding was carried out with an Arburg 250-75-270D machine (Arburg Maschinenfabrik Hehl and Soehne GmbH and Co. KG, Lossburg, Germany). The barrel was heated in four zones, with temperatures set at 110, 120, 120, 120°C from feed to nozzle. The mould temperature was controlled by the HB-150 M temperature controller, set at 20°C for all runs. A pressure transducer in the mould cavity was used to record mould pressure directly. The volumetric flow rate of the injection was standardized at approximately 8×10^{-6} m^3 s^{-1}; this produced a maximum wall shear rate of 566 s^{-1} in the 3 mm diameter entry nozzle. An alternative volumetric flow rate of 2×10^{-6} m^3 s^{-1} was also used for one set of tests. The mould cavity used was a 15 × 20 × 65 mm bar; typical products are shown in Fig. 2. The sprue entered on the top surface at one end of the mould cavity. The outlet diameter was 4 mm; the sprue had a 2° taper.

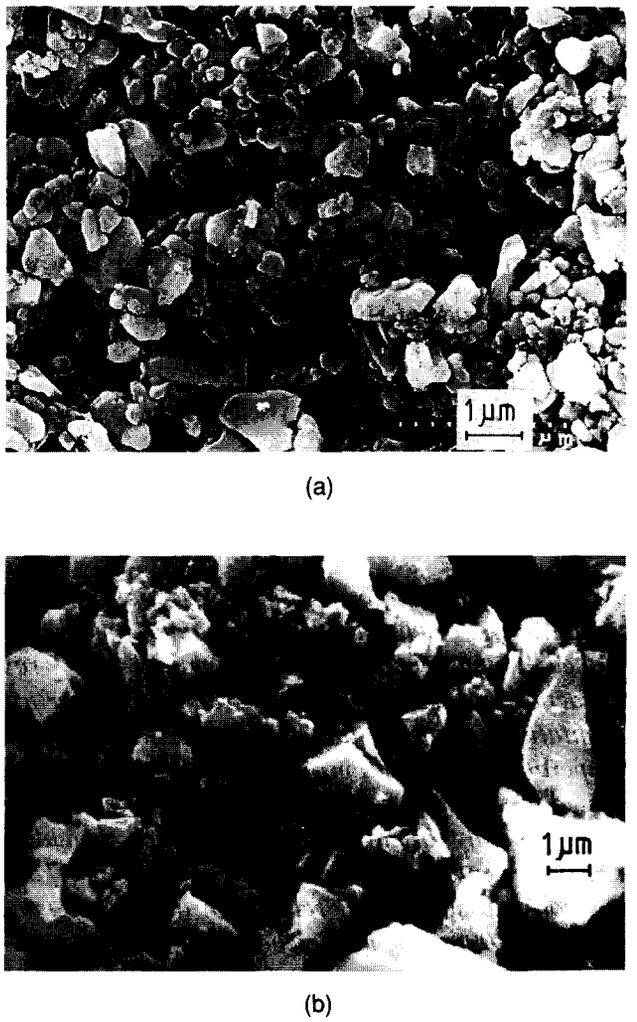

Fig. 1. SEM photographs of the powders used for injection moulding: (a) Baco RA107LS, (b) F1500.

2.3 Characterization

The orientation of the binder was measured with an annealing method as used by Allen and Bevis.[1] The injection-moulded bar was cut along the axial direction into sections as shown in Fig. 3(a). The sprue end 'e' was discarded and the samples u, c, b, s_1, s_2 studied. Annealing was carried out at

Table 1. Moulding compositions

	RA107LS		*F1500*		*Density (kg m^{-3})*
	wt%	*vol%*	*wt%*	*vol%*	
Alumina	88·79	65·0	86·48	60·0	3970
EVA	3·75	11·5	4·53	13·2	951
PW	3·75	11·9	4·53	13·6	916
SA	1·83	6·3	2·23	7·2	941
DBP	1·85	5·3	2·23	6·0	1042

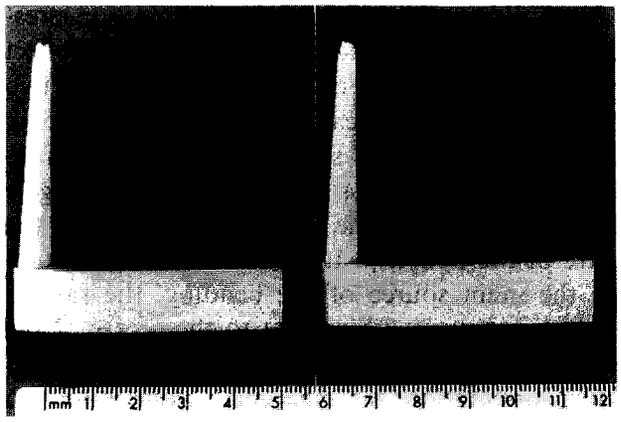

Fig. 2. Injection-moulded bars prior to sectioning.

120°C . Under these conditions the bars were normally curved and the degree of bending in these sections was expressed by bending curvature k:

$$k = 8y/l^2 \tag{1}$$

where y and l are the deformation and the length of the bar respectively (Fig. 4).

The samples for X-ray diffraction are shown in Fig. 3(b). The measurements were carried out on small thin sections, approximately 12 × 18 mm. The particle orientation was measured by X-ray diffraction using Cu K_α radiation. Step scanning was used with steps of 0·05° 2θ (2 s per step).

Alumina is a tabular material due to the prominent development of the basal pinacoid (0 0 1).[13] This implies that the diffraction intensity of (0 0 1) should be the most intense and therefore be the most useful in the characterization of orientation. However, the diffraction intensity I is given by:

$$I = |F_{hkl}|^2 \rho \left(\frac{1 + \cos^2 2\theta}{\sin^2\theta \cdot \cos^2\theta} \right) = |F_{hkl}|^2 \rho L_0 \tag{2}$$

where θ is the Bragg angle, ρ is the multiplicity factor, L_0 is the Lorentz polarization factor and

$$F_{hkl} = \sum_1^n f_n e^{2\pi i(hU_n + kV_n + kW_n)} \tag{3}$$

where f_n is the atomic scattering factor and U_n, V_n and W_n are the associated atomic coordinates in the unit cell. The results show that the diffraction intensity from (0 0 1) is not detectable and so cannot be used for orientation analysis. Therefore the (1 1 0) diffraction, which is perpendicular to (0 0 1), was used for the orientation analysis.

The degree of orientation was calculated by using a modified Lotgering method.[5] In this technique, the degree of orientation C was obtained from

$$C = \frac{P - P_0}{1 - P_0} \tag{4}$$

and

$$P = \frac{\Sigma I(00l)}{\Sigma I(hkl)} \tag{5}$$

where $\Sigma I(00l)$ and $\Sigma I(hkl)$ are the sums of the diffraction intensities of $(00l)$ and (hkl) respectively, and P_0 stands for P obtained from a theoretically randomly packed powder sample. If $\Sigma I(00\,l) >> \Sigma I(hkl)$, $h \neq 0$, $k \neq 0$ or $\Sigma I(00\,l) << \Sigma I(hkl)$, $h \neq 0$, $k \neq 0$, C will be either close to zero or 1. In other words, it is not sensitive to changes of the intensities of $(00l)$ diffraction and considerable error will arise. To avoid this, the normalized intensity $I(hkl)$ was used:

$$I(hkl) = I(hkl) / [I_0(hkl) / I_0(\max)] \tag{6}$$

where $I_0(hkl)$ and $I_0(\max)$ are the intensities of the (hkl) and maximum diffraction planes in the randomized powder. For a randomized powder sample they are equal to a constant as shown in the JCPDS files. As discussed above, in this work $P = I(1\,1\,0)/\Sigma I(1\,1\,l)$ was used and since (1 1 0) is perpendicular to (0 0 1), increasing C indicates a decrease in the orientation of the (0 0 1) plane.

3 Results and Discussion

3.1 The relaxation of binder

The style of curvature in samples cut from the moulded bar and annealed at 120°C for 24 h is shown schematically in Fig. 4. The degrees of

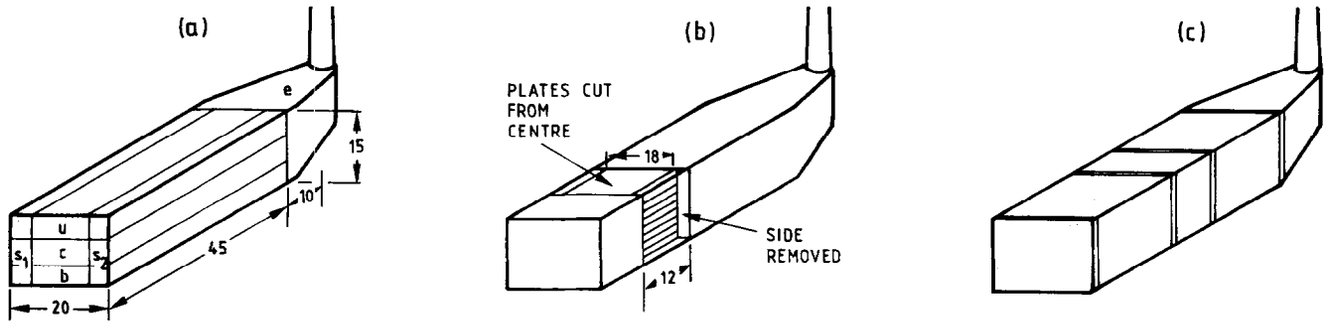

Fig. 3. (a) Samples for the annealing test. The letters indicate the sample nomenclature and the lines represent the saw cuts; dimensions in mm. (b) Samples for X-ray diffraction measurements; dimensions in mm. (c) As (b), but samples cut perpendicular to the long axis of the bar.

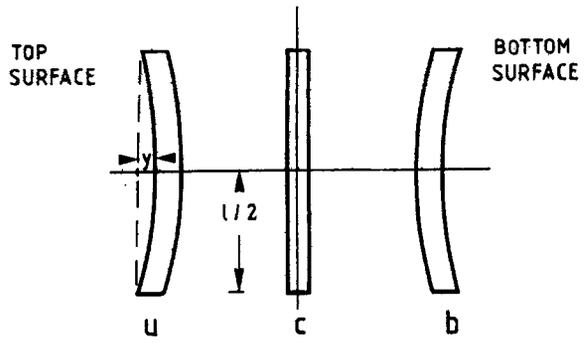

Fig. 4. Schematic representation of samples of RA107LS annealed at 120°C for 24 h; u and b are the top and bottom sections of the sample, respectively, c is the centre section.

curvature, calculated using eqn (1), are shown in Table 2, where the negative sign is used to distinguish concave bending with respect to the centre line of the original body before sectioning.[12] Samples cut from the centre of the bar, i.e. samples c, remained straight.

Table 2. Bending curvature of samples after annealing at 120°C for 24 h

Sample	*Injection pressure (MPa)*	*Injection flow ($m^3 s^{-1}$)*	*Curvature (m^{-1})*
RA107LS			
c	60	8×10^{-6}	0
u			-0·9
b			-1·25
s_1			-1·0
s_2			-0·95
RA107LS			
c	40	8×10^{-6}	0
u			-0·8
b			-1·0
s_1			-0·85
s_2			-0·6
RA107LS			
c	20	8×10^{-6}	0
u			-0·4
b			-1·85
s_1			-0·85
s_2			-0·8
RA107LS			
c	20	2×10^{-6}	0
u			-0·65
b			-1·2
s_1			-1·0
s_2			-1·3
F1500			
c	60	8×10^{-6}	0
u			0
b			0
s_1			0
s_2			0
F1500: RA107LS = 2:1 by weight			
c	60	8×10^{-6}	0
u			-1·5
b			-1·8
s_1			-0·9
s_2			-0·6

As shown in Table 2, changes in injection pressure and moulding speed had no significant effect on the mode or degree of curvature. There are two main reasons which cause the sample to bend: relaxation of residual stress and binder orientation. The residual stress distribution would largely be compressional at the surface and tensile in the centre of the body.[14,15] If residual stress relaxation was the main source of the bending, the sample would be convex with respect to the centre of the original body. This suggests that relaxation of binder orientation was the main contributor to bending of the samples, the binder becoming oriented at the wall along the bar axis, i.e. parallel to the predominant flow direction. No bending was observed in samples cut from bars fabricated with F1500. Thus it can be concluded that the shape and alignment of the non-spherical grains in the RA107LS powder contributed in some way to the alignment and stretching of the binder phase.

3.2 The orientation of particles

The degree of particle orientation in components fabricated with RA107LS was measured from moulded bars cut both parallel and perpendicular to the long axis of the bar. Parallel to the axis, two sets of samples were cut [Fig. 3(b)] at 20 mm and 40 mm from the closed end of the mould. The particle orientation results are shown in Fig. 5. The top surface was taken as the datum. Here, the particles tended to pack randomly, with the calculated degree of orientation being near to zero. The degree of orientation is maximized between 2 and 3 mm from the surface. Here the (001) planes in the particles predominantly lie parallel to the mould surface. In the centre, the degree of orientation remains high but is reversed thereby becoming positive, which indicates that the (001) plane tends to lie perpendicular to the mould surface

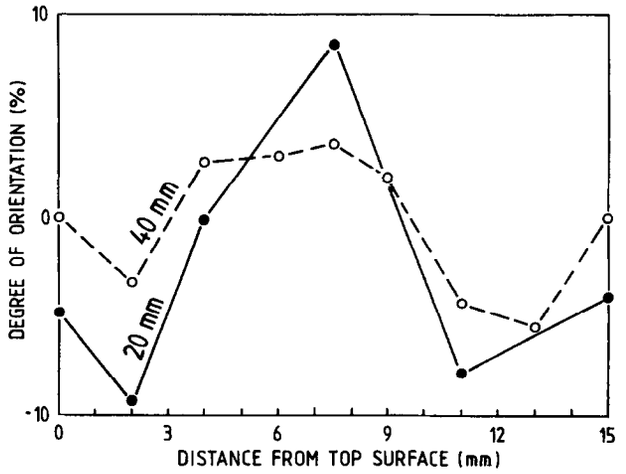

Fig. 5. Particle orientation determined by X-ray diffraction analysis in RA107LS components with respect to depth through the sample, for sample sections 20 and 40 mm from the closed end of the mould.

Table 3. Degree of orientation in cross-section perpendicular to the flow direction

Distance to end of mould cavity (mm)	*Degree of orientation (%)*
50	-5·85
30	-5·85
20	-2·85
0	-3·3

and the predominant direction of mould flow. The orientation measured from sections cut perpendicular to the bar axis [Fig. 3(c)] is shown in Table 3. Each position shows average orientation predominantly parallel to the mould surface, i.e. a negative degree of orientation. This shows that the (001) plane in the particles tends to align parallel to the mould surface. This occurs because, in averaging the measurements over the cross-section, the zone with this orientation occupies the greatest cross-sectional area.

The orientation of particles in a bar moulded with F1500 powder mixture is shown in Fig. 6 (line a) for half the body section. At all the positions, the degree of orientation was close to zero, suggesting that the particles were packed randomly. This probably reflects the less plate-like nature of the powder. For comparison, a mixture of F1500 and RA107LS powders in the ratio 2:1 by weight and with the same binder content as the RA107LS compositions was prepared, the mould pressure again being 60 MPa. The degree of orientation is shown in Fig. 6 (lines b and c, duplicate samples). Comparing this with pure F1500 components, the slightly increased orientation was believed to be attributable to the RA107LS. In an additional experiment, the RA107LS powder was

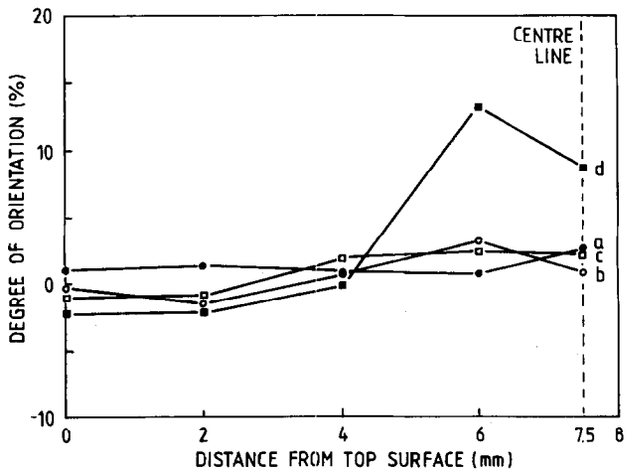

Fig. 6. Particle orientation determined by X-ray diffraction with respect to depth through the sample for different compositions: (a) F1500; (b) and (c) duplicates of a mixture of F1500 and RA107LS powder = 2:1 (by weight); (d) RA107LS powder ball-milled for 72 h. All sample sections 20 mm from the closed end of the mould.

ball-milled for 72 h with the hope of improving its sphericity and subsequently moulded under the same conditions as initially used. The results of orientation studies on these materials are again shown in Fig. 6, line d; milling did not appear to significantly reduce orientation. Scanning electron microscopy observations suggested that milling did not change the powder morphology significantly.

3.3 The cooling of material in the cavity and sprue

3.3.1 Temperature distribution in the mould cavity

The temperature distribution in the moulded bar was calculated using the finite difference method. In order to simplify the calculation, the bar was treated as a bar of infinite length. However, since the area of the cross-section is much smaller than the surface area of the side, the error will be small. The aim of this calculation was not to quantify the processing–structure relationship, but aid in the analysis of the orientation mechanism.

The general equation for heat transfer in two dimensions is

$$\frac{\partial^2 T}{\partial x^2} + \frac{\partial^2 T}{\partial y^2} = \frac{1}{\alpha} \cdot \frac{\partial T}{\partial t} \tag{7}$$

where α is the thermal diffusivity which is a function of temperature T; t denotes time.[16] Since the mould temperature is thermostatically controlled, it was assumed that the mould temperature remained constant, and an energy balance technique[16] was used for the boundary nodes with a convective boundary condition. The rate of heat flow Q_{om} to a node o from its neighbouring node m gives rise to the following equation

$$\sum_m Q_{om} = \rho_0 C_{\rho_0} V \frac{T_0(t + \Delta t) - T_0(t)}{\Delta t} \tag{9}$$

where ρ_0, C_{ρ_0} and V are density, specific heat and node volume, respectively. For an internal node m

$$Q_{om} = \frac{kA_{om}}{L_{om}} (T_m - T_0) \tag{10}$$

For the mould surface node, the rate of heat flow from the mould to the component is

$$Q_{om} = khA_{om}(T_m - T_0) \tag{11}$$

where k and h are the thermal conductivity and the heat transfer coefficient, respectively. A_{om} is the element area perpendicular to the direction between node o and m; L_{om} is the distance between node o and m, T_m is the mould temperature.

A computer program was written to calculate the node temperatures. The thermal properties of the moulding material and the heat transfer coefficient between the body and the mould were taken from previous work.[17,18]

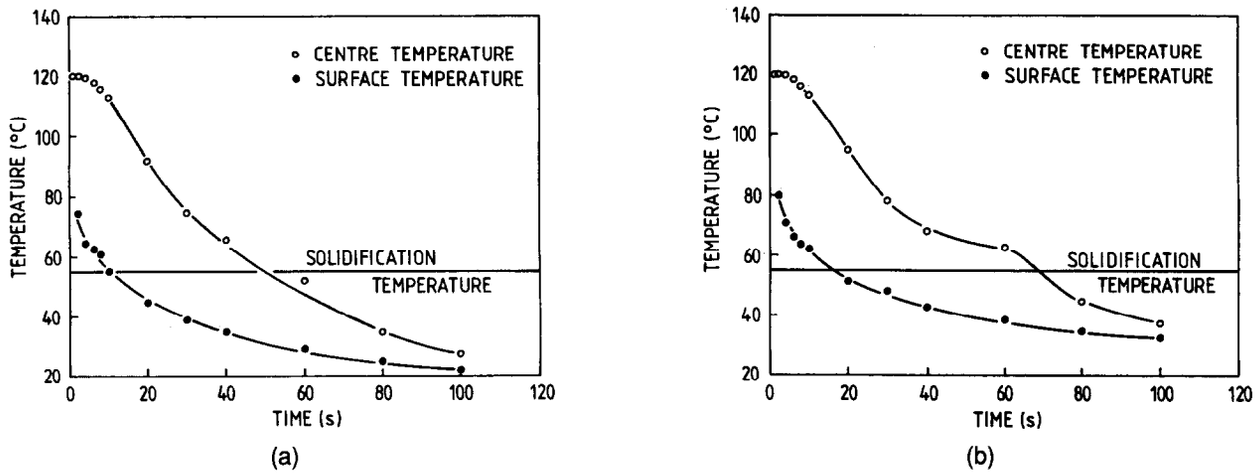

Fig. 7. Cooling of the moulded material at the surface and in the centre: (a) mould temperature 20°C; (b) mould temperature 30°C.

The surface and centre temperatures in the body during cooling are plotted in Figs 7(a) and (b). It can be seen that when mould temperature is increased from 20 to 30°C, the melt solidification time increases by ~5 and 20 s at the surface and at the centre of the body, respectively. The model also indicates that there is a large temperature difference between mould surface and body centre during cooling. When the mould temperatures are set at 20 and 30°C, the centre of the body takes 40 and 55 s, respectively, longer than the surface to become solid. The relationships between the thickness of the solidification layer and temperature for the two mould temperatures are shown in Fig. 8. It can be seen that the layer thickness increases at a similar rate for the first 20 s after which there is a divergence, with the thickness of the 30°C mould increasing more slowly for the next 20 s. The two systems are fully solid after approximately 70 s.

3.3.2 Temperature distribution in the sprue

The cooling of melt in the sprue was calculated by a finite difference method.[18] The calculation was carried out on sprues of different diameters. The temperatures in the centre of the sprue are shown in Fig. 9. The model indicates that the sprue diameter has a large influence on the solidification time. On the other hand, mould temperature has little effect. For the sprue of 4 mm diameter used in this research, the model predicts that the sprue solidification time will increase from 12 to 13·5 s

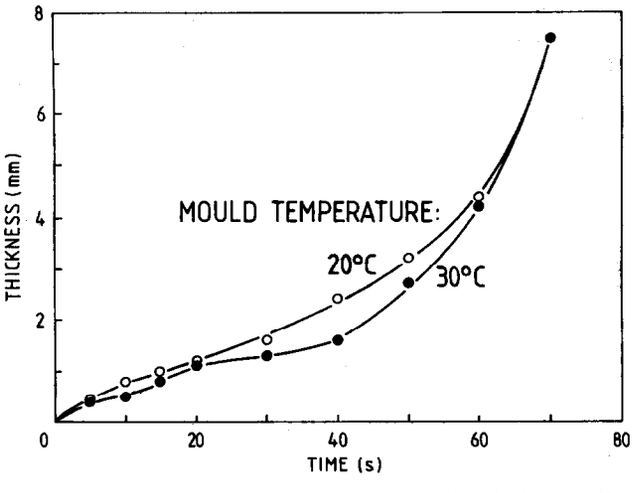

Fig. 8. Solidification of the moulded material during cooling with respect to distance from the mould surface.

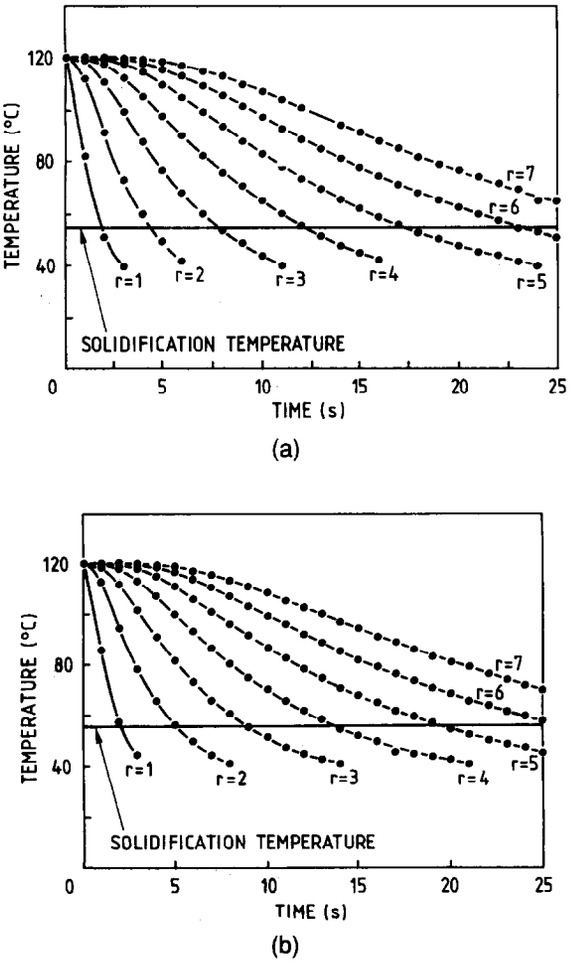

Fig. 9. Temperature in the centre of the sprue with respect to time during cooling: (a) mould temperature 20°C; (b) mould temperature 30°C. The sprue radius is r (mm).

as the mould temperature increases from 20 to 30°C. This implies that, when the sprue becomes solid, the solid layer thickness of the solidifying body will be less than 1 mm at both mould temperatures. It can thus be shown that when the sprue is solid, 75 vol% of the mould body remains molten.

3.4 The development of binder and particle orientation

Binder orientation is the combined result of the alignment of the molecule in the direction of applied shear stress, the relaxation of this alignment caused by Brownian movement[19] and restriction by packed particles. Any increases in shear stress such as the increase of injection pressure and injection speed would increase the orientation. High material temperature and large cross-section allow increased time for Brownian relaxation; the degree of orientation will decrease, which is consistent with the observations. In practice, the influence of these parameters seems to be small in the samples generated within this study.

The mould filling sequence is shown in Fig. 10. It can be seen that the melt enters the mould as a stream initially to form a coil, later flowing to uniformly fill the mould fully from one end to the other. From Figs 8 and 9, when the mould was just filled (2 s) the solidified layer in the body was less than 0·5 mm thick. At this point the model suggests that the sprue was still molten. The materials employed tended to shrink during cooling and under this situation the melt flow to the cavity would continue under the injection pressure. At this point the material in the cavity would be under shear. However, the shear stress varies with the position, the largest shear stress occurring in the boundary layers between the solidified surface and the melt front. It is in this region where the largest degree of orientation was observed. After the sprue solidified, no external pressure and shear stresses acted on the body. At this point the model estimates that 75 vol% of material in the mould cavity was still molten,which took a further 55 s to fully solidify. It appears the binder was not fully relaxed (returned to its original structural configuration) during this period in the RA107LS bodies. The binder was fully relaxed in the F1500 samples, though both solidify at similar rates. This suggests that the relaxation rate of the binder is affected by the properties of the powders, in particular the morphology.

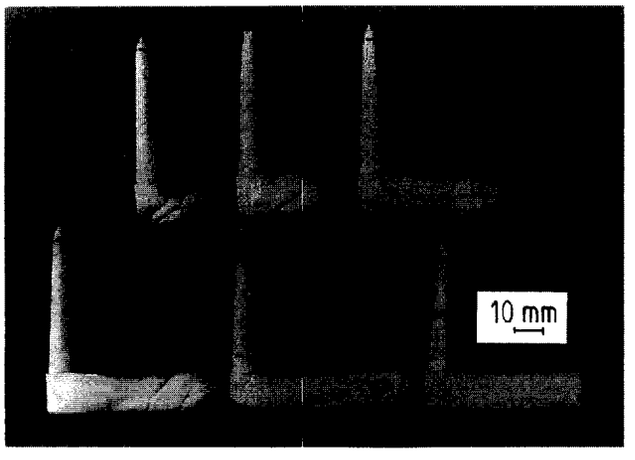

Fig. 10. Mould filling behaviour during injection moulding; the samples were formed in separate short-shot injection experiments.

The relaxation of the binder was observed over 24 h during the annealing test. No bending was found in any F1500 mouldings regardless of the annealing time. Samples of moulded RA107LS became progressively relaxed with time. However, after 5 h, bending was negligible. This is consistent with particle orientation and particle size having significant effects on the binder orientation and relaxation.

Mason and co-workers[20,21] analysed the motion of particles of various shapes in a flowing suspension. In a concentrated suspension (>10 vol% powder), particles interact frequently and move irregularly, and motion aligns the particles because of particle–particle interactions.[20] The orientation occurs more rapidly at higher powder concentrations with the final state depending on the concentration and the particle size. The magnitude of the shear stress has no effect on the final state of alignment.[21] In the current study, where the powder concentration was higher than 60 vol%, the initially injected material was randomly oriented; during the period of bulk mould filling prior to complete sprue solidification, the melt flowed into the centre of the cavity with a parabolic flow front giving the observed axial orientations. Similar flow forms have been described by Robinson[22] in ceramic extrusion. The orientation pattern of the plate-like particles in RA107LS reflects the flow and appears to be independent of moulding pressure and the speed. This observation is consistent with the work of Mason.

4 Conclusion

Studies on annealed bars sliced from thick section injection-moulded samples reveal the orientation of the organic binder used in the injection-moulded ceramic body. A modified calculation method for X-ray analysis was used to estimate the degree and mode of particle orientation, and this confirms that plate-like particles orient during the moulding operation. The organic binder phase in the mixes containing fine plate-like powders tended to orient in the predominant direction of

flow in the sub-surface of the body. In such systems the relaxation rate was slow. At a depth of 2–3 mm from the body surface, the particles tended to lie with the plane (001) parallel to the mould surface whereas, at the centre of the mould, this plane tended to lie perpendicular to the mould surface.

A finite difference method was used to calculate the temperature distribution in the mould cavity and the sprue. The results aided the analysis of flow and formation of oriented structure. It has been shown that the orientation is not affected by the moulding pressure or the moulding speed but is dominated by the shear flow during the final stages of mould filling. The oriented particle has a significant effect on binder orientation and the relaxation mechanisms of the binder system.

Acknowledgement

The authors are grateful to the EPSRC for support of the IRC foundation programmes.

References

1. Allen, P. & Bevis, M., 1. The production of void-free thick section injection-flow mouldings, 2. Preferred orientation and residual stress measurement. *Plast. Rubber Process. Applic.*, **3** (1983) 331–336.
2. Cox, R. W. & Williamson, W. O., Differential shrinkage of clays and bodies caused by particle-orientation and its significance in testing-procedure. *Trans. Br. Ceram. Soc.*, **57** (1958) 85–101.
3. Igarashi, H., Matsunaga, K., Taniai, T. & Okazaki, K., Dielectrical and piezoelectric properties of grain-oriented $PbBi_2Sb_2O_9$ ceramics. *Am. Ceram. Soc Bull.*, **57** (1978) 815–817.
4. Watanabe, H., Kimura, T. & Yamaguchi, T., Particle orientation during tape casting in fabrication of grain-oriented bismuth titanate. *J. Am. Ceram. Soc.*, **72** (1989) 289–293.
5. Kimura, T., Yoshimoto, T., Lida, N., Fujita, Y. & Yumaguchi, T., Mechanism of grain orientation during hot-pressing of bismuth titanate. *J. Am. Ceram. Soc.*, **72** (1989) 85–89.
6. Hoffmann, M. J., Nagel, A., Greil, P. & Petzon, G., Slip casting of SiC-whisker-reinforced Si_3N_4. *J. Am. Ceram. Soc.*, **72** (1989) 765–769.
7. Tsao, I. & Danforth, S. C., Injection-mouldable ceramic composites: compounding behaviour, whisker degradation and orientation. *Am. Ceram. Soc. Bull.*, **72** (1993) 55–64.
8. Chou, Y. S. & Green, D. J., Silicon carbide platelet/alumina composites: 1. Effect of forming technique on platelet orientation. *J. Am. Ceram. Soc.*, **75** (1992) 3346–3352.
9. German, R. M., *Powder Injection Moulding*. Metal Powder Industries Federation, Princeton, NJ, 1990, pp. 3–22.
10. Merhar, J. R., A personal perspective on metal injection moulding. *Int. J. Powder Metall.*, **27** (1991) 105–106.
11. Zhang, T. & Evans, J. R. G., Relaxation effects in large injection moulded ceramic bodies. *J. Eur. Ceram. Soc.*, **12** (1993) 51–59.
12. Zhang, T., Blackburn, S. & Bridgwater, J., Defects during debinding and sintering caused by particle orientation in ceramic injection moulding. *J. Mat. Sci.*, in press.
13. Phillips, F. C., *An Introduction to Crystallography*, Halsted Press, New York, 1977, pp. 89–94.
14. Kostic', B., Zhang, T. & Evans, J. R. G., Measurement of residual stress in injection-moulded ceramics. *J. Am. Ceram. Soc.*, **75** (1992) 2773–2778.
15. Mills, N. J., Computation of residual stress in extruded and injection moulded products. *Plast. Rubber Process. Applic.*, **3** (1983) 181–188.
16. Croft, D. R. & Lilley, D. G., *Heat Transfer Calculations using Finite Difference Equations*. Applied Science Publications, London, 1977, pp. 14–39.
17. Zhang, T. & Evans, J. R. G., Thermal properties of ceramic injection moulding suspensions in liquid and solid states. *J. Eur. Ceram. Soc.*, **6** (1989) 303–309.
18. Zhang, T. & Evans, J. R. G., Calculation of temperature distributions during the solidification stage in ceramic injection moulding. *J. Am. Ceram. Soc.*, **75** (1992) 2260–2267.
19. Rubin, I., *Injection Moulding Theory and Practice*. Wiley-Interscience, London, 1972, pp. 251–263.
20. Karnis, A., Goldsmith, H. L. & Mason, S. G., The kinetics of flowing dispersion, 1. Concentrated suspension of rigid particles. *J. Colloid Interface Sci.*, **22** (1996) 531–553.
21. Ancurowski, E., Cox, R. G. & Mason, S. G., The kinetics of flowing dispersions, IV. Transient orientation of cylinders. *J. Colloid Interface Sci.*, **23** (1967) 547–562.
22. Robinson, G. C., Extrusion defects. In *Ceramic Processing Before Sintering*, eds G. Y. Onoda & J. L. L. Hench. John Wiley & Sons, New York, 1978, pp. 391–401.